

2016

An Empirical Estimate of Post-LGM Grounding-Event Duration in Eastern Ross Sea: Implications from a Comparison with Constraints from New Radiocarbon Dates

Benjamin Krogmeier

Louisiana State University and Agricultural and Mechanical College

Follow this and additional works at: https://digitalcommons.lsu.edu/gradschool_theses



Part of the [Earth Sciences Commons](#)

Recommended Citation

Krogmeier, Benjamin, "An Empirical Estimate of Post-LGM Grounding-Event Duration in Eastern Ross Sea: Implications from a Comparison with Constraints from New Radiocarbon Dates" (2016). *LSU Master's Theses*. 2275.

https://digitalcommons.lsu.edu/gradschool_theses/2275

This Thesis is brought to you for free and open access by the Graduate School at LSU Digital Commons. It has been accepted for inclusion in LSU Master's Theses by an authorized graduate school editor of LSU Digital Commons. For more information, please contact gradetd@lsu.edu.

AN EMPIRICAL ESTIMATE OF POST-LGM GROUNDING-EVENT DURATION IN EASTERN ROSS SEA:
IMPLICATIONS FROM A COMPARISON WITH CONSTRAINTS FROM NEW RADIOCARBON DATES

A Thesis

Submitted to the Graduate Faculty of
Louisiana State University
Agricultural and Mechanical College
In the partial fulfillment of the
requirements for the degree of
Master in Science

in

The Department of Geology and Geophysics

by

Benjamin J. Krogmeier
B.S., Central Michigan University, 2014
May 2016

TABLE OF CONTENTS

ABSTRACT	iii
INTRODUCTION	1
METHODS.....	4
RESULTS.....	7
DISCUSSION.....	14
CONCLUSIONS.....	18
REFERENCES	19
APPENDIX - SUPPLEMENTARY METHODS.....	22
VITA	26

ABSTRACT

The West Antarctic Ice Sheet (WAIS) advanced to the outer shelf during the Last Glacial Maximum (LGM) before beginning a rapid retreat to the inner shelf. In the Whales Deep paleo-ice-stream trough, subsurface and geomorphologic evidence shows that grounding-line retreat was interrupted by at least five pauses in the area between the shelf edge and the middle shelf. During the pauses, an overlapping cluster of backstepped grounding zone wedges (GZWs) was deposited. Each GZW represents a grounding event, i.e., a time interval during which the grounding-line position was relatively stable. Seismic correlation and isopach mapping show that the cluster has a total volume of $5.34 \times 10^{11} \text{ m}^3$. Based on our estimate of modern deformation-till flux at Bindschadler Ice Stream, we infer that when the WAIS was grounded at the middle shelf, the paleo-sediment flux would have been as high as $\sim 5.36 \times 10^8 \text{ m}^3\text{a}^{-1}$. Using this paleo flux, the middle-shelf grounding events would have had a duration of $\sim 995 \pm 493$ years. In contrast, radiocarbon dates show that the middle-shelf grounding events had a duration of at least 3200 years. The comparison shows that in the absence of radiocarbon control, our empirical approach provides a reasonable first-order estimate of grounding event duration.

INTRODUCTION

Since the LGM, the WAIS has retreated more than 1000 km from the outer continental shelf to its current interglacial configuration in Ross Sea (e.g., Anderson et al., 1992). Much research continues to focus on the WAIS retreat history because this evidence might reveal what factors disturb grounding-line stability and trigger retreat of grounded ice that returns ice volume to the global ocean. Fortunately, the erosional and depositional products of the relatively-recent retreat are well preserved, being mostly intact at the seafloor in the form of low-relief bathymetric features (e.g., Wellner et al., 2006) and transgressive successions in core (e.g., Domack et al., 1999). In some sectors, the stratigraphic evidence shows that, once it had begun, the early retreat of grounded ice did not occur by a steady southward migration of the grounding-line. Instead, the grounding-line position stabilized several times. The geomorphologic evidence shows that these early pauses were sufficiently long for seismically-resolvable GZWs to be constructed. GZWs are asymmetrical low-relief features with a gentle landward-dipping surface leading to a steeper basinward-dipping termination.

For what duration was grounding-line retreat interrupted? Several studies have hinted at the possible durations of the modern grounding events (e.g., Anandakrishnan et al., 2007) but these studies are limited because they are usually based on a 2D consideration of GZW dimensions and sediment volume. Other strategies have relied on post-LGM chronologies around the continent. Strictly speaking, the results of most ice-sheet-retreat studies constrain the date with which the ice-shelf calving front moved passed at a particular core location. Unfortunately, it has proven to be difficult to date the duration of pre-modern grounding events because the onset of the grounding event is not constrained due to the following two

challenges. Firstly, the overall retreat chronology is poorly constrained because of a paucity of *in situ* carbonate and uncertainties regarding radiocarbon dating in the Southern Ocean.

Secondly, even where good-quality radiocarbon dates are available, the current number of dated core sites is too coarsely spaced along the axes of the paleo-trough systems to constrain the durations of the discrete grounding events (as required by the backstepping successions of large and small GZWs).

A recent study by Bart and Owolana (2012) explored a strategy that attempted to avoid these two chronology problems by using an approach that did not explicitly rely on radiocarbon dates. They mapped GZW sediment volume and estimated ice-stream sediment flux to calculate a grounding-event duration for the middle shelf GZW in the Glomar Challenger Basin paleo-ice-stream trough. The GZW volume was mapped in detail with seismic data but their sediment-flux estimate required three key assumptions concerning: 1) the duration of the modern GZW at Kamb Ice Stream; 2) the volume of the modern GZW at the mouth of the Kamb Ice Stream; and 3) the larger dimensions of the drainage basin when the entire WAIS was grounded on the middle shelf of Glomar Challenger Basin. Because the assumptions are not confirmed with data, it remains difficult to directly evaluate whether or not their estimated grounding-event durations are accurate. In other words, the Bart and Owolana (2012) study should be considered speculative.

Here we present results of a new method to calculate the middle-shelf grounding event duration for the Whales Deep Basin, (i.e., the paleo-ice-stream trough immediately to the east of Glomar Challenger Basin) (Figure 1). This new approach more directly relies on the observed

sediment flux at the base of the Bindschadler Ice Stream (Kamb, 2001) and hence avoids some of the assumptions made by Bart and Owolana (2012).

In the time since our empirical study of grounding-event duration of Whales Deep basin began, DeCesare et al. (in prep.) generated radiocarbon dates from the outer shelf portion of the paleo-ice stream trough. These radiocarbon dates provide an opportunity to determine if our new empirical approach of estimating grounding-event duration is accurate.

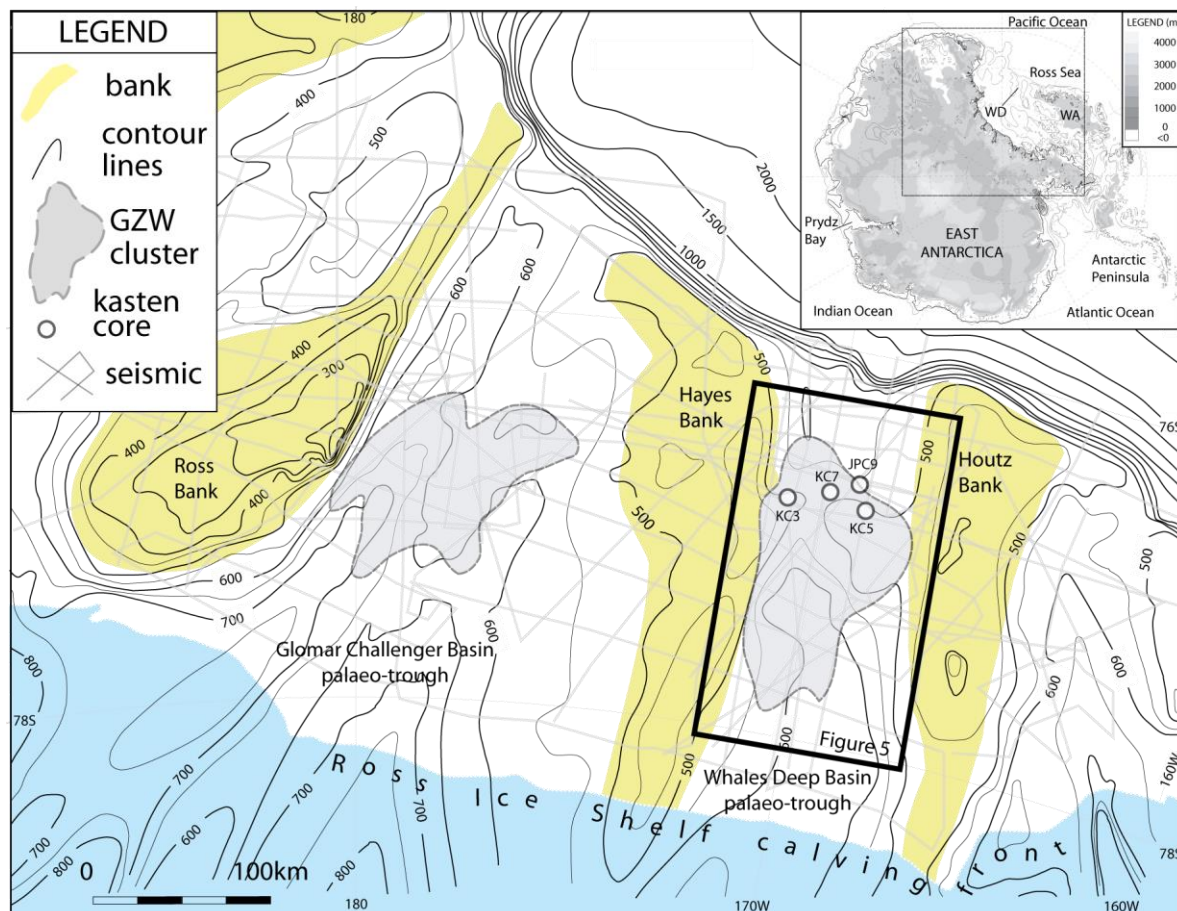


Figure 1. Bathymetric map of the eastern Ross Sea showing paleo-ice-stream troughs on the continental shelf including regional seismic line locations. The mid-shelf shaded units bound by dashed lines show the middle shelf GZWs in Glomar Challenger and Whales Deep basins. The yellow shapes are bathymetric highs, which separate each trough. Modified from Bart and Owolana (2012).

METHODS

Our study involved three parts designed to calculate the duration of the post-LGM grounding events in the Whales Deep paleo-ice-stream trough. The first part concerned mapping the extent of the GZWs by seismic correlation. We used high-resolution single- and multi-channel seismic profiles from six surveys that include strike and dip profiles. Three regional dip-oriented transects from the axis of Whales Deep were acquired during NBP1502B. The interpreted seismic profiles were used to create an isopach contour map of the GZW cluster showing the thickness distribution in milliseconds of two-way travel time. The contour map was converted to depth and then used to calculate the GZW volume using a sediment velocity of 1750 ms^{-1} based on seismic-derived velocity estimates of high-latitude glacial sediments (Sætem et al., 1992b; Cochrane et al., 1995).

The second part involved creating an empirical estimate of sediment flux (Q) for the Whales Deep Basin paleo-ice-stream trough. The sediment-flux estimate we generated was based on previous direct borehole observations of the modern-day Bindschadler Ice Stream. Data presented by Kamb (2001) indicated that deforming-basal till moved past a borehole site near the grounding-line at a velocity of 292 m a^{-1} . We assumed that the deforming-till layer has an average thickness of 6.5 m (Rooney et al., 1987) across the entire 150,000 m width of streaming ice (Rignot et al., 2011). On these bases, we estimated that the Bindschadler Ice Stream has a modern deforming-basal-till flux (Q_{3DM}) of $2.8 \times 10^8 \text{ m}^3 \text{ a}^{-1}$. Our flux estimate does not include sediment flux from basal ice as its volume is likely not preserved within the GZWs.

This modern 3D flux was then used to calculate an average erosion rate (i.e., sediment yield, S , in $\text{m}^3 \text{ m}^{-2} \text{ a}^{-1}$) for the modern Bindschadler Ice Stream drainage area. Average inferred

sediment yield (S), or the volume of sediment eroded from the drainage basin per unit area each year ($2.3 \times 10^{-3} \text{ m}^3\text{m}^{-2}\text{a}^{-1}$), was quantified using equation (1).

$$S (\text{m}^3\text{m}^{-2}\text{a}^{-1}) = Q_{3\text{DM}} (\text{m}^3\text{a}^{-1}) / \text{Drainage area (m}^2\text{)} \quad (1)$$

This modern sediment yield was applied to the larger drainage basin area that existed when the WAIS was grounded on the middle shelf (Figure 2) to calculate a paleo-3D sediment flux ($Q_{3\text{DP}}$) for the Whales Deep basin. The paleo 3D sediment flux should apply to the deposition of the middle shelf GZW cluster.

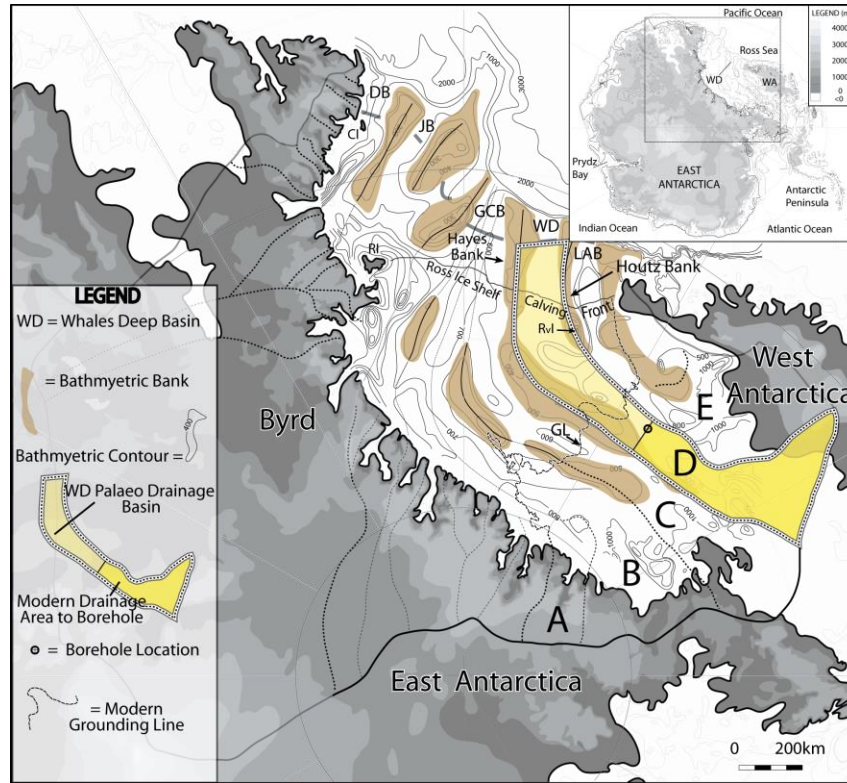


Figure 2. Map of Antarctica showing subglacial elevation. The light yellow shade shows the paleo-ice sheet drainage for Whales Deep Basin when ice existed on the middle continental shelf. The darker yellow portion extending to the current ice sheet grounding-line shows the modern drainage area for the Bindschadler Ice Stream as defined by Rignot et al. (2011). Ice streams labeled A-E are Mercer, Whillans, Kamb, Bindschadler, and Macayeal respectively. Rvl=Roosevelt Island, RI=Ross Island. Inset includes map symbols of important features. Modified from Bart and Owolana (2012).

Thirdly, we used the paleo-3D sediment flux (Q_{3DP}) to estimate the duration of the middle-shelf grounding events using the GZW cluster sediment volume and sediment flux estimates (from parts 1 and 2, respectively) as shown in Equation (2):

$$d = v_s / Q_{3DP} \quad (2)$$

where d is the duration in years (a), v_s is GZW sediment volume (in m^3), and Q_{3DP} is the Whales Deep 3D sediment flux (in m^3a^{-1}). Our empirical estimate of grounding-event duration was then compared to the duration of the grounding events as can be deduced from new radiocarbon dates (DeCesare et al., in prep.).

RESULTS

Seismic stratigraphy, mapped limits and sediment volume (v_s) of the post-LGM middle shelf GZW cluster

Stratigraphic super-position via seismic correlations show that a GZW cluster overlies a regional unconformity that can be projected as a seafloor reflection at the shelf edge into the subsurface across the middle- and the inner-shelf portions of the Whales Deep trough. At the outer shelf, the multibeam survey shows that the sea-floor unconformity is marked by megascale glacial lineations (MSGs). MSGs indicate that streaming grounded ice once reached its maximum extent on the shelf edge (Bart and Greenwood, in prep). Mosola and Anderson (2006) proposed that these subglacial features formed during the LGM. Radiocarbon dates of *in situ* foraminifera isolated from sub-ice-shelf sediments overlying the unconformity confirm that the shelf-edge grounding event came to an end after the LGM (DeCesare et al., in prep.).

On the middle shelf, the backstepping cluster of GZWs overlying this LGM unconformity is composed of at least 5 trough-confined GZWs (Figure 3). The individual wedges are labeled GZW 1 through 5 from oldest to youngest. The pattern with which the WAIS grounding-line backstepped was such that parts of GZWs 1, 2 and 3, and all of GZW5 are exposed at the seafloor.

In the area between the middle-shelf bathymetric saddle and the shelf edge, the topsets and foresets of GZWs 1 through 3 are evident on the multibeam survey (Figure 3). The first four GZWs are comparatively thin (20 msec TWTT, i.e., 15 m) and hence beyond those areas where the downlap limits are traceable on the multibeam survey, their extents are difficult to trace across the study area because the top and base reflectors cannot be seismically resolved.

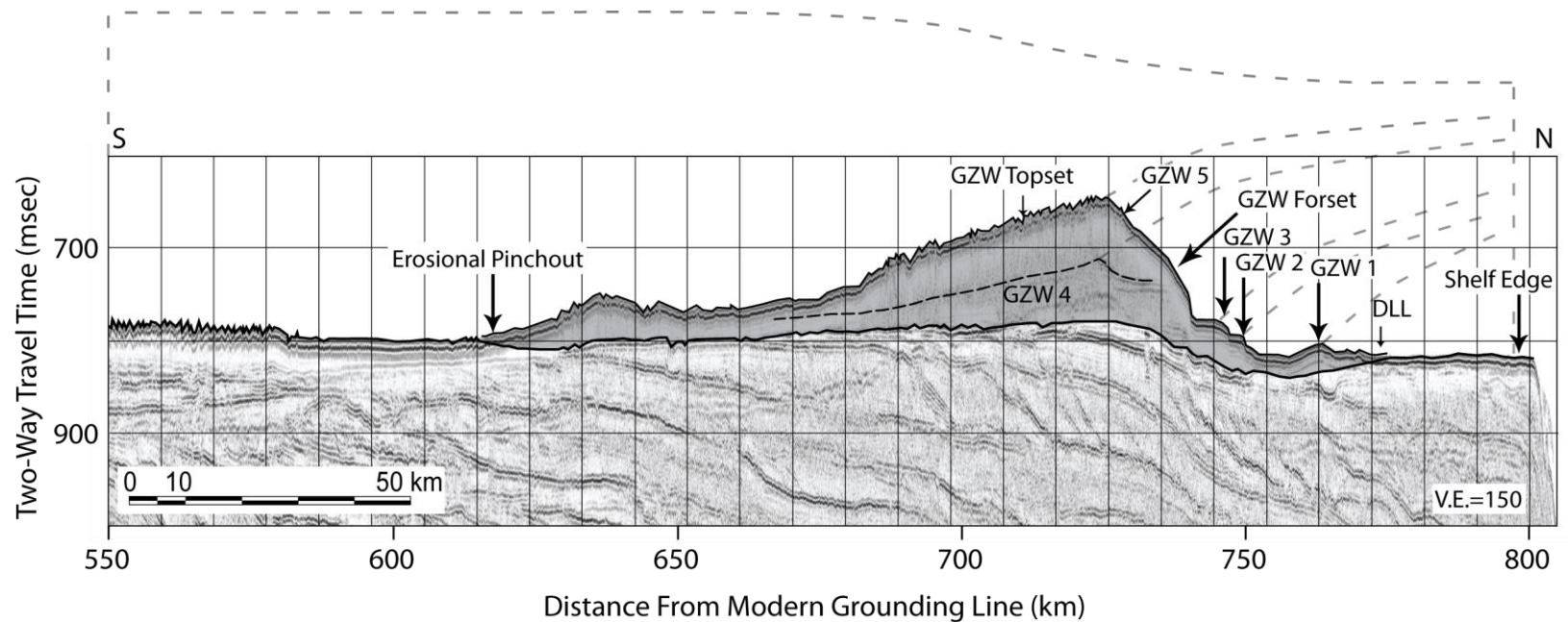


Figure 3. Geometry of the middle shelf GZW cluster imaged by a portion of the strike-oriented seismic profile NBP1502B-03 within the Whales Deep Basin shaded in grey. GZW thins southward terminating in depositional pinchout. The lower extent of the unit rests upon the sharply imaged Brown Unconformity, while the upper extent is the Grey Unconformity (Bart, 2004). DLL = downlap limit. Location of seismic line shown on Figure 4.

Seismic data shows that GZW4 is everywhere buried by what must have been a slight re-advance of grounded ice during the construction of GZW5 (Figure 3).

The north end of the bathymetric saddle corresponds to the approximate grounding-line position for GZW5. The correlations of strike- and dip-oriented seismic transects show that the GZW cluster has a large thickness distributed over the central part of Whales Deep Basin between the flanks of the Hayes and Houtz banks (Figure 4). In other words, the mapping shows that the middle-shelf GZW cluster is trough confined.

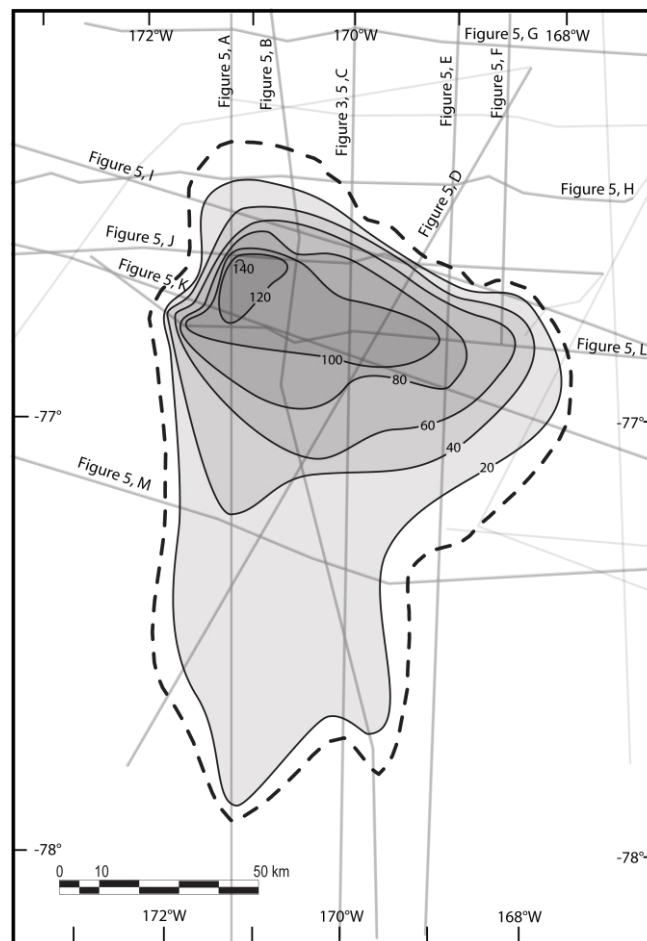


Figure 4. Isopach map of the Whales Deep Basin GZW cluster based on seismic and multibeam data compilation. The map extent of the GZW cluster is also shown in Figure 1. This map extent replaces the grey unit shown in Bart and Cone (2012). Figure includes transects of seismic surveys collected in the area. Bold lines indicate portions of seismic transects shown in Figure 5.

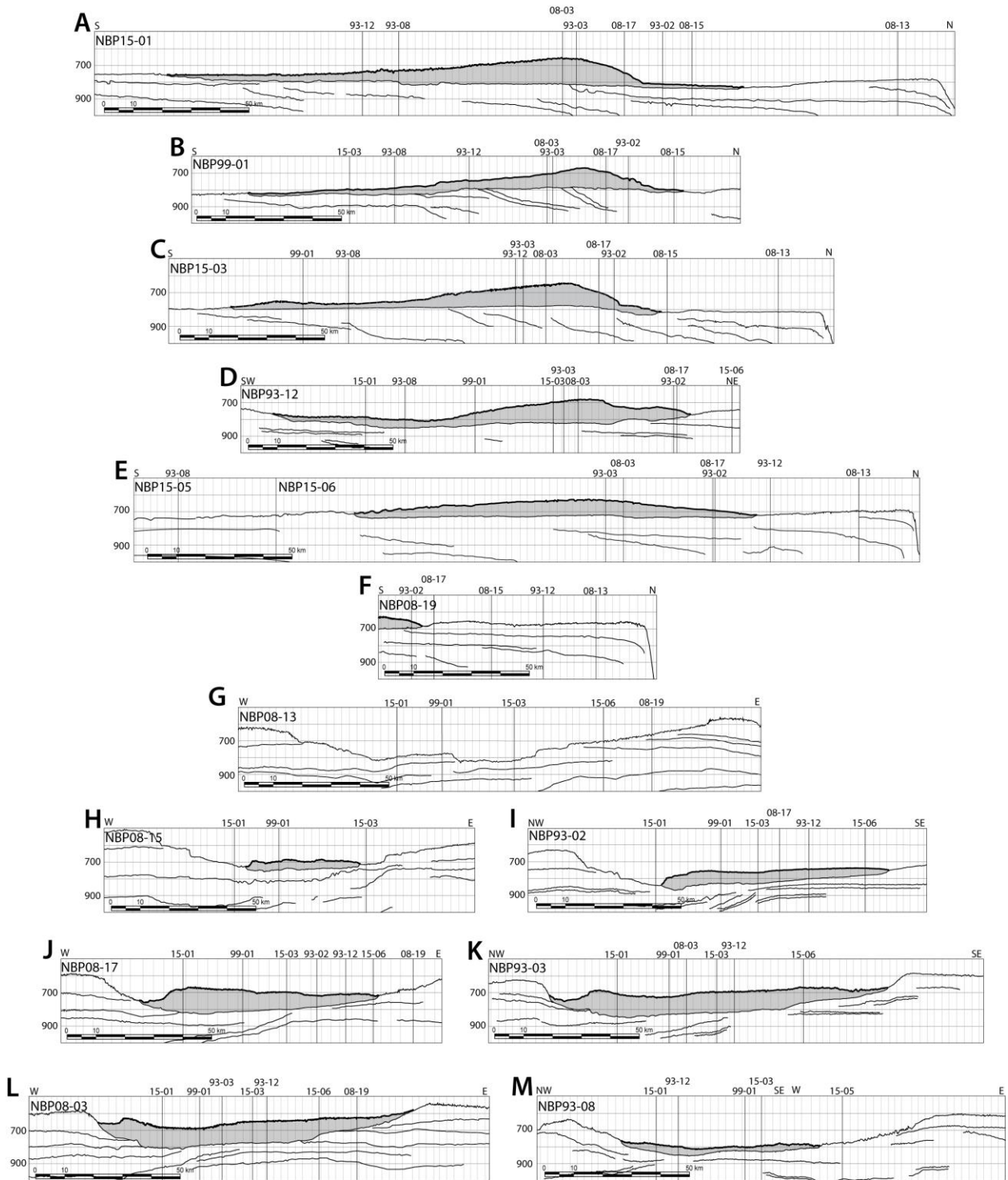


Figure. 5. Line drawings of seismic interpretation highlighting the base and top of the Whales Deep GZW cluster. Profiles A-F show dip orientation moving west to east while G-M show oblique and strike orientation of the trough. The bold line shows the uppermost surface of the GZW cluster while the shaded grey portion identifies the wedges at depth. V.E.= 65

The isopach map (Figure 4) highlights that the cluster thickens gradually from the inner shelf to a tight east-west trend of contours at the middle-shelf saddle. At the bathymetric saddle, the cluster thickens to 140 m but thins abruptly to a depositional pinchout limit on the outer shelf. Volumetric analysis of the isopach map reveals that the GZW cluster contains a sediment volume of $5.34 \pm .25 \times 10^{11} \text{ m}^3$ (Table 1).

Table 1. Summarized results and dimensions for the Whales Deep modern and paleo basins. Sediment flux (Q) is reported in 2D ($\text{m}^3\text{m}^{-1}\text{a}^{-1}$) and 3D (m^3a^{-1}) where appropriate. Modern drainage area represents the area of the Bindschadler Ice Stream as outlined by Rignot and Thomas (2002) up to borehole 98-3. Paleo drainage area represents the modern drainage area and the area between borehole 98-3 and the basinward extent of the GZW cluster.

	Sediment Flux Q (m^3)	Drainage Area (m^2)	Yield S ($\text{m}^3\text{m}^{-2}\text{a}^{-1}$)	GZW Volume (m^3)	Duration d (a)
Borehole 98-3	$1898 \text{ m}^3\text{m}^{-1}\text{a}^{-1}$	-	-	-	-
Modern	$2.8 \times 10^8 \text{ m}^3\text{a}^{-1}$	1.23×10^{11}	2.3×10^{-3}	-	-
Empirical	$5.36 \times 10^8 \text{ m}^3\text{a}^{-1}$	2.32×10^{11}	2.3×10^{-3}	$5.34 \pm .25 \times 10^{11}$	955 ± 493
Radio Carbon	$1.62 \times 10^8 \text{ m}^3\text{a}^{-1}$	2.32×10^{11}	7.0×10^{-4}	$5.34 \pm .25 \times 10^{11}$	3200 ± 800

The upper and lower bounding surfaces of the GZW cluster are an amalgamation of reflections at different stratigraphic levels corresponding to the individual GZWs (Figure 3). Where an older GZW is overlain by younger GZW, the underlying (i.e., buried) topset reflection is weak and discontinuous. Landward of the GZW saddle, the upper topset unconformity of GZW5 is a seafloor reflection that was last eroded at the end of the grounding event that constructed GZW5.

The pinchout limit of the GZW cluster (Figure 1) in the southern end of the Whales Deep basin is defined by subglacial erosion at the upper-bounding surface of GZW5 (Figure 5, A).

Internally, the individual GZWs are reflection free.

Modern and paleo yield (S), and sediment flux (Q) estimates for the Bindschadler Ice Stream

Kamb (2001) showed that deformation accounts for 80% of modern ice stream motion (i.e., 80% of 365 m a^{-1}) of the Bindschadler Ice Stream. A tethered-stake experiment showed that deformation till moves past the bore hole with a velocity of $\sim 0.8 \text{ m d}^{-1}$ (or 292 m a^{-1}). The total thickness of the deformation till was not measured at the bore hole. Elsewhere, seismic studies have shown that deformation till thicknesses range from 2 to 15 m (e.g., Rooney et al., 1987, Blankenship et. al., 1987). Based on observations across several transects of streaming ice summarized by Rooney et al. (1987), deformation-till thickness averages $\sim 6.5 \text{ m}$. These data suggest that there may be as much as $1898 \text{ m}^3 \text{ m}^{-1} \text{ a}^{-1}$ (Table 1) of deformation till moving past Bindschadler Ice Stream borehole 98-3 (Figure 1). When the 2D borehole deformation-till flux is extrapolated across the 150-km trough width, the modern sediment flux (Q_{3DM}) is estimated to be $2.85 \times 10^8 \text{ m}^3 \text{ a}^{-1}$ (Table 1). Average inferred sediment yield (S) (i.e., the volume of sediment eroded from the drainage basin per unit area each year) was $2.3 \times 10^{-3} \text{ m}^3 \text{ m}^{-2} \text{ a}^{-1}$ (Table 1).

Extrapolation of this sediment yield over the paleo drainage area results in a paleo sediment flux, Q_{3DP} , of $5.36 \times 10^8 \text{ m}^3 \text{ a}^{-1}$ (Table 1). Using equation (2), we calculate that the duration of the middle-shelf grounding events was 995 ± 493 years (Table 1). The error for the grounding-event-duration estimate includes a $\pm 2 \text{ m}$ uncertainty associated with the TWTT measurements of the GZW cluster's upper and lower bounding seismic reflections. The

seismic-based estimate of average deformation-till thickness has a ± 1.5 m uncertainty. The error also includes $\pm 50 \text{ ms}^{-1}$ uncertainty in the velocity used to convert the isopach from TWTT to depth.

Radiocarbon constraints on the middle-shelf grounding event duration

Radiocarbon dates from the middle shelf at JPC9 (Figure 1) shows that sub-ice-shelf sediments was accumulating over the LGM diamict by at least 14.7 ± 450 cal kyr BP (DeCesare et al., in prep.). This statement relies on stratigraphic superposition as revealed by seismic stratigraphic relationships (Figure 3) and multibeam bathymetry. Also, on the middle shelf, radiocarbon dates from KC3, KC5 and KC7 (Figure 1) show that proximal diamict sediment was deposited on the stratigraphically-younger GZW5 foreset until at least 11.5 ± 350 cal kyr BP. The combination of radiocarbon dates and stratal relationships requires that the entire middle-shelf cluster of GZWs was deposited within at least 3200 ± 800 years (Table 1).

DISCUSSION

The empirical estimate of grounding-event duration is shorter than the actual duration required by radiocarbon dates

The empirical-estimate of grounding-event duration is of the same order as that deduced from radiocarbon dates albeit 3.2 times shorter (i.e., 995 ± 493 years versus 3200 ± 800 years) (Table 1). The radiocarbon-based estimate is obviously superior to the empirical estimate. In other words, our new strategy overestimated sediment flux (and hence significantly under-estimates grounding-event duration for the Whales Deep paleo drainage system). The errors we estimated for the empirical study must be far larger than we inferred. On this basis, we revise our duration estimate to be 955 ± 2245 years.

Possible sources of error in the empirical estimate of grounding-event duration

In the absence of radiocarbon control, the empirical method provides a reasonable first-order estimate of grounding event duration. However, one or more of the assumptions we made to generate the empirical estimate of sediment flux must be incorrect. The key assumptions concerned the thickness, width, velocity and un-interrupted flow of the deformation-till layer. The values we used for these variables were derived from the averages of modern instantaneous observations of ice-stream systems. However, data from some previous studies suggests that the vertical thickness and horizontal width of the deformation till layer (across the cross-section of the ice stream) is likely to vary over time and from ice stream to ice stream (Engelhardt and Kamb, 1998; Kamb, 2001). It is not possible to uniquely know how the sediment flux varied during the grounding event. However, the mismatch between empirical and radiocarbon-based estimates of grounding-event duration indicates that the

modern instantaneous observations are not representative of the average sediment flux for the entire middle-shelf grounding event at Whales Deep.

A lower average flux value could have been associated with any combination of a thinner, narrower (i.e., cross-section width), or slower flowing deformation-till layer. We note that our empirical estimate assumed that deformation till moved with the same velocity from top to base. The borehole observations only pertain to the velocity of the upper few centimeters (Kamb, 2001). Repeat satellite-interferometric synthetic-aperture-radar data mapping (Rignot et al., 2011) also shows that ice velocity varies spatially and temporally across Antarctica. In addition, ice streams can experience intervals of stagnation on the order of centuries (Shabtaie and Bentley, 1987; Retzlaff and Bentley, 1993). We assumed that the ice streaming was accomplished by dilatational till deformation but fast flow may also occur by basal sliding (e.g., Engelhardt and Kamb, 1998). However, during intervals of either ice-stream deceleration, stagnation or shift to streaming by basal sliding, sediment flux would diminish or cease. There is little direct information concerning the degree to which paleo-ice-stream shifted back and forth between active and stagnant states by till deformation versus basal sliding. For our empirical estimate of sediment, we assumed no deceleration or stagnation of the ice stream. To get a better sediment flux average, one would need to know how the various parameters varied during the grounding event.

Comparison with other estimates of grounding-event duration and flux

In the case of the Whales Deep middle shelf GZW cluster, the chronologic constraints indicate that the empirical estimate of paleo sediment flux generated using the strategy we employed is too high. In retrospect, the paleo flux we used should be considered a maximum

for at least two reasons. Firstly, we assumed that deformation till had a uniform 6.5-m thickness across the entire 150-km width of the trough uniformly moving at 292 ma^{-1} through the entire duration of the grounding event. Secondly, we assumed that the entire volume of deformation till flux was captured in the GWZ cluster, i.e., no significant volume of suspension-mode sediment was generated by deformation-till flux process. Given that the sediment flux was too high, the empirical strategy we utilized underestimated the duration of the middle-grounding event in the Whales Deep paleo-ice-stream trough (equation 2).

Bart and Owolana (2012) proposed that the middle-shelf grounding event in Glomar Challenger Basin could have been associated with either WAIS advance leading up to the LGM or WAIS retreat post-dating the LGM. The radiocarbon dates from DeCesare et al. (in prep.) strongly favor the latter scenario. For their post-LGM scenario, Bart and Owolana (2012) estimated that the Glomar Challenger middle-shelf grounding event had a minimum duration of 1400 years, i.e., roughly half as long as that for the Whales Deep basin. Given the large-than-expected error associated with the empirical study of Whales-Deep grounding-event duration, the Bart and Owolana (2012) empirical estimate for the Glomar Challenger Basin should be considered with caution. The similar middle shelf positions suggest that the Glomar Challenger and Whales Deep middle shelf grounding events may have formed synchronously. It is not possible to determine whether the middle shelf event in Glomar Challenger Basin was as long as the >3200 years for the Whales Deep middle shelf.

Many other studies have commented on the presence of GZWs and hinted at their association with grounding-line stability of some duration (e.g., Larter and Vanneste, 1995; Alley et al., 2007; Anandakrishnan et al., 2007; Dowdeswell et al., 2008). In no case other than

DeCesare et al. (in prep.) is the actual duration of an Antarctic grounding event well constrained by radiocarbon dates. GZWs have been imaged and identified in each trough across the Ross Sea (Anderson *et al.*, 1992; Shipp and Anderson, 1997; Shipp *et al.*, 1999). The positioning and size of GZWs vary across the margin, but the largest trough-confined GWZs are of a volume comparable to the GZW cluster found in Whales Deep (Shipp et al., 1999; Howatt and Domack, 2000; Bart et al., 2000; Bart and Owolana, 2012). The apparently similar sediment volume for large GZWs in adjacent drainage systems, does not necessarily suggest similar grounding-event duration because sediment flux is a complex function of many variables (i.e., deformation-till velocity and thickness/width, and ice-stream drainage area).

Modern and pre-modern grounding-event durations have been suggested to last several decades to centuries (e.g., Alley et al., 2007; Anandakrishnan et al., 2007; Dowdeswell et al., 2008; Livingstone et al., 2012). The shorter durations were calculated as a function of modern and paleo estimated Antarctic 2D sediment fluxes ranging between 100 and 1000 m³m⁻¹a⁻¹ (Alley et al., 1987, 1989; Tulaczyk et al., 2001; Shipp et al., 2002; Bougamont and Tulaczyk, 2003; Christofferson et al., 2010). These short-duration grounding-event estimates maybe problematic because they are based on a 2D approach applied to a 3D feature deposited within a trough-basin of a specific width. Moreover, on the basis of radiocarbon constraints, the average 2D sediment flux rate required to build the post-LGM GZW cluster at the Whales Deep middle shelf would be 1600 m³m⁻¹a⁻¹ ($Q_{3DP}/\text{width of GZW cluster}$). Conversely, using our empirical approach, the average required 2D sediment flux would be 5300 m³m⁻¹a⁻¹. In other words, the radiocarbon-based 2D sediment flux rate is thus 1.6 higher than those suggested by previous studies. This comparison suggests that previous estimates of 2D flux may be too low.

CONCLUSIONS

Our empirical estimate of sediment flux for the Whales Deep paleo ice stream predicts that the GZW cluster would have taken ~ 1000 years to deposit. Radiocarbon constraints however indicate that the grounding-events were ≥ 3200 years, i.e., significantly longer. The comparison of the two grounding-event estimates suggests that the assumptions we applied (based on instantaneous modern ice-stream sediment flux) do not apply for the entire duration of the middle-shelf grounding events in Whales Deep Basin. The actual sediment flux for the paleo Bindschandler Ice Stream may have been lower for several reasons, but it is not possible to know which of our assumptions should be adjusted. Further refinements of empirical methodology are needed to produce grounding-event estimates as robust as that provided by radiocarbon constraints. However, in the absence of radiocarbon dates, we proposed that using the empirical method of calculating GZW duration provides a useful first-order estimate.

REFERENCES

- Alley, R.B., Anandakrishnan, S., Dupont, T.K., Parizek, B.R., Pollard, D., 2007. Effect of sedimentation on ice-sheet grounding-line stability. *Science*, vol. 315, pp. 1838-1841.
- Alley, R.B., Blankenship, D.D., Rooney, S.T., Bentley, C.R., 1987. Till beneath Ice Stream B, 3, Till deformation: Evidence and implications. *Journal of Geophysical Research*, vol. 92, pp. 8921-8929.
- Alley, R.B., Blankenship, D.D., Rooney, S.T., Bentley, C.R., 1989. Sedimentation beneath ice shelves - the view from ice stream B. *Marine Geology*, vol. 85, pp. 101-120.
- Anandakrishnan, S., Catania, G.A., Alley, R.B., Horgan, H.J., 2007. Discovery of till deposition at the grounding line of Whillans Ice Stream. *Science*, vol. 315, pp. 1835-1838.
- Anderson, J.B., Shipp, S., Bartek, L.R., Reid, D.E., 1992. Evidence for a grounded ice sheet on the Ross Sea continental shelf during the late Pleistocene and preliminary paleo drainage reconstruction. In: Elliott, D.H. (Ed.), *American Geophysical Union Antarctic Research Series, Contributions to Antarctic Research III*, vol. 57, pp. 39-62.
- Bart, P.J., Anderson, J.B., Trincardi, F., Shipp, S.S., 2000. Seismic data from the Northern basin, Ross Sea, record extreme expansions of the east Antarctic ice sheet during the late Neogene. *Marine Geology*, vol. 166, pp. 31-50.
- Bart, P.J., Owolana, B., 2012. On the duration of West Antarctic Ice Sheet grounding events in Ross Sea during the Quaternary. *Quaternary Science Reviews*, vol. 47, pp. 101-115.
- Bartek, L.R., Andersen, J., and Oneacre, T.A., 1997. Ice Stream Troughs and Variety of Cenozoic Seismic Stratigraphy Architecture from a High Southern Latitude Section: Ross Sea, Antarctica. In T.H. Davies, T. Bell, A.K. Cooper, H. Josenhans, L. Polyak, A. Solheim, M.S. Stoker, and J.A. Stravers (Eds.), *Glaciated Continental Margins: An Atlas for Acoustic Images*, Chapman and Hall, New York, pp. 250-253.
- Bartek, L.R., Henrys, S.A., Anderson, J.B., and Barrett, P.J., 1996. Seismic Stratigraphy of McMurdo Sound, Antarctica: Implications for Glacially Influenced Early Cenozoic Eustatic Change? *Marine Geology*, vol. 130, pp. 79-98.
- Blankenship, D.D., Bentley, C.R., Rooney, S.T., and Alley, R.B., 1987, Till beneath Ice Stream B: 1. Properties derived from seismic travel times: *Journal of Geophysical Research*, vol. 92, pp. 8903-8911.
- Bougamont, M., Tulaczyk, S., 2003. Glacial erosion beneath ice streams and ice-stream tributaries: constraints on temporal and spatial distribution of erosion from numerical simulations of a West Antarctic ice stream. *Boreas*, vol. 32, pp. 178-190.
- Christoffersen, P., Tulaczyk, S., Behar, A., 2010. Basal ice sequences in Antarctic ice streams: Exposure of past hydrological conditions and a principle mode of sediment transfer. *Journal of Geophysical Research*, vol. 115: F03034.

- Cochrane, G.R., De Santis, L., Cooper, A.K., 1995. Seismic Velocity expression of glacial sedimentary rocks beneath Ross Sea from sonobouy seismic-refraction data. In: Cooper, A.K., Barker, P.F., Brancolini, G. (Eds.), *Geology and Seismic Stratigraphy of the Antarctic Margin*. Antarctic Research Series, vol. 68, pp. 261-270.
- DeCesare, M., and Bart, P.J., 2016 (in prep), West Antarctic Ice Sheet retreat in the eastern Ross Sea – a Post-LGM evidence from foraminiferal radiocarbon dates.
- Domack, E.W., Jacobsen, E.A., Shipp, S., Anderson, J.B., 1999. Late Pleistocene-Holocene retreat of the West Antarctic Ice Sheet system in the Ross Sea: part 2- Sedimentologic and stratigraphic signature. *GSA Bulletin*, vol. 111, pp. 1517-1536.
- Dowdeswell, J.A., Ottesen, D., Evans, J., Ó Cofaigh, C., Anderson, J.B., 2008. Submarine glacial landforms and rates of ice-stream collapse. *Geology*, vol. 36, pp. 819–822.
- Engelhardt, H., and Kamb, B., 1998. Basal sliding of Ice Stream B, West Antarctica, *J. Glacial.*, vol. 44, pp. 223-230.
- Howatt, I.M., and Domack, E.W., 2003. Reconstruction of western Ross Sea palaeo-ice-stream grounding zones from high-resolution acoustic stratigraphy. *Boreas*. doi:10.1080/03009480310001038.
- Kamb, B., 2001. Basal zone of the West Antarctic ice streams and its role in lubrication of their rapid motion. In: Alley, R.B., Bindshadler, R.A. (Eds.), *The West Antarctic Ice Sheet: Behavior and Environment*. Antarctic Research Series, AGU, Washington, D.C, vol. 77, pp. 157-201.
- Larter, R.D., Vanneste, L.E., 1995. Relict subglacial deltas on the Antarctic Peninsula outer shelf. *Geology* vol. 23, pp. 33-36.
- Livingstone, S.J., O Cofaigh, C., Stokes, C.R., Hillenbrand, C.D., Vieli, A., Jamieson, S.S.R., 2012. Antarctic palaeo-ice streams. *Earth-Science Reviews*, vol. 111, pp. 90-128.
- Mosola, A.B., Anderson, J.B., 2006. Expansion and rapid retreat of the West Antarctic Ice Sheet in eastern Ross Sea: possible consequence of over-extended ice streams? *Quaternary Science Reviews*, vol. 25, pp. 2177-2196.
- Retzlaff, R., and C. R. Bentley, 1993. Timing of stagnation of ice stream - C, West Antarctica, from short-pulse radar studies of buried surface crevasses, *J. Glaciology*, vol. 39, pp. 553–561.
- Rignot, E., Mouginot, J., Scheuchl, B., 2011. Ice flow of the Antarctic ice sheet. *Science*, vol. 333, pp. 1427-1430.
- Rignot, E., and Thomas, R., 2002. Mass Balance of polar ice sheets. *Science*, vol. 297, pp. 1502-1506.
- Rooney, S.T., Blankenship, D.D., Alley, R.B., and Bentley, C.R., 1987. Till beneath Ice Stream B. 2. Structure and continuity, *Geophysical Research*, vol. 92, pp. 8913-8920.

- Sættem, J., Rise, L. & Westgaard, D. A. 1992b. Composition and properties of glacigenic sediments in the southwestern Barents Sea. *Marine Geotechnology*, vol. 10, pp. 229–255.
- Shabtaie, S., and C. R. Bentley, 1987. West Antarctic ice streams draining into the Ross Ice Shelf—Configuration and mass balance, *J. Geophys. Res.*, vol. 92, pp. 1311–1336.
- Shipp, S., Anderson, J.B., 1997. Grounding zone wedges on the Antarctic continental shelf, Ross Sea. In: Davies, T.A., Josenhans, H., Polyak, L., Solheim, A., Stoker, M.S., Stravers, J.A. (Eds.), *Glaciated Continental Margins, An Atlas of Acoustic Images*. Chapman & Hall, London, pp. 104–105.
- Shipp, S., Anderson, J., Domack, E., 1999. Late Pleistocene-Holocene retreat of the west Antarctic ice-sheet system in the Ross Sea: part 1 – geophysical results. *GSA Bulletin*, vol. 111, pp. 1486-1516.
- Shipp, S.S., Wellner, J.S., Anderson, J.B., 2002. Retreat signature of a polar ice stream: sub-glacial geomorphic features and sediments from the Ross Sea, Antarctica. In Dowdeswell JA, Ó Cofaigh C (Eds.). *Glacier-Influenced Sedimentation on High-Latitude Continental Margins*, Geological Society, London, Special Publication, vol. 203, pp. 277–304.
- Tulaczyk, S.B., Scherer, R.P., Clark, C.D., 2001. A ploughing model for the origin of weak tills beneath ice streams: a qualitative treatment. *Quaternary International*, vol. 86, pp. 59-70.
- Wellner, J.S., Heroy, D.C., Anderson, J.B., 2006. The death mask of the Antarctic ice sheet: comparison of glacial geomorphic features across the continental shelf: *Geomorphology* vol. 75, pp. 157-171.

APPENDIX - SUPPLEMENTARY METHODS

Data Collection, Mapping, and GZW Volume (v_s)

The extent of the GZW cluster associated with the LGM in the Whales Deep trough was mapped using over 3000 km of seismic data from four surveys which showed the basinward extent, i.e., the depositional downlap limit of the GZWs. The seismic surveys included multi- and single-channel seismic data. All surveys utilized a generator-injector airgun source. The Polar Duke survey (PD90) was collected in 1990 aboard the *Polar Duke RVIB*. The other four surveys were collected from the *Nathanial B. Palmer RVIB* and included NBP93-08, NBP99, NBP08, NBP1502B. Data acquisition parameters for PD90, NBP93-08, and NBP99 are reported in Bartek et al., (1996), Bartek et al., (1997), and Mosola and Anderson (2006) respectively. The data quality is good. Hard copies of these data were utilized for the other surveys. The seismic data with the best resolution was acquired during NBP1502B. During this survey, three regional dip-oriented transects were acquired along the entire axis of the Whales Deep Basin from the Ross Ice Shelf calving front to the shelf edge. A single harmonic generator-injected airgun with a 90 in³ volume was used as the seismic source fired at a 5-second interval. The 24-channel seismic streamer had a total length of 75m and contained three grouped hydrophones spaced at 3.125m. The source and streamer were towed 60m and 105m astern of the transom respectively. The average ship speed was 5 knots, which equated to a shot spacing of 3.25m. The seismic reflections were recorded without filtering.

The composite top and base of the GZW cluster was correlated across all profiles. The bounding surfaces of the individual GZWs are not mappable as regional seismic reflections. In particular, the topset surfaces of GZWs cannot be reliably mapped in the places where the unit

is buried by a younger GZW. The base of the GZW cluster is a regional unconformity that extends to the shelf edge and defines the top of the LGM deposits. The upper surface of the GZW cluster is the seafloor reflection over much of the area south of the middle shelf bathymetric saddle. The difference in the two-way travel time (in milliseconds) between the top and base of the middle shelf GZW cluster was measured at an approximate spacing of 2.5 kilometers along every seismic transect. Thickness in meters was determined using Equation (3):

$$T = \frac{1}{2}(\text{TWTT}) * V_s \quad (3)$$

where T is the sediment thickness in meters, and V_s is sediment velocity in meters per second. We use a sediment velocity of 1750 m/s based on seismic-derived velocity estimates of Ross Sea sediments (Cochrane et al., 1995).

The isopach contour map we created was used to estimate the total sediment volume using ArcGIS software. First, a triangular irregular network (TIN) surface was created to represent the seafloor based on the spacing of contours. This program then calculated and summed the sediment volume between each triangle in the network and the 0m contour representing the limit of the GZW sediment.

Yield (S) and Flux (Q)

On the basis of the flux estimates, Q_{3DM} , and the area of the Bindschadler Ice Stream drainage basin (from Rignot and Thomas, 2002), sediment yield (S), or the volume of sediment eroded from the drainage basin per unit area each year ($\text{m}^3/\text{m}^2/\text{a}$), was quantified using equation (4):

$$S \text{ (m}^3\text{m}^{-2}\text{a}^{-1}\text{)} = Q_{3\text{DM}} \text{ (m}^3\text{a}^{-1}\text{)} / \text{Drainage area (m}^2\text{)} \quad (4)$$

Drainage area estimates for modern flux calculations were based on parameters outlined by Rignot and Thomas (2002) extending to the Bindschadler Ice Stream borehole. A drainage area for the paleo-ice-stream that deposited the middle shelf GZW cluster was calculated by adding the modern drainage area to the area of the trough lying between the Bindschadler Ice Stream borehole and the paleo grounding-line on the middle shelf of the Whales Deep paleo-ice stream trough. This was done using the measure tool in ArcGIS software to create a polygon outlining the extent of the entire paleo drainage area and finding the area of the polygon.

Duration Error

We cannot estimate the error in duration based on the uncertainties quantified for each variable directly from equation 2 because some factors are not directly used for in the duration formula. For example, we estimate a seismic sediment velocity of $1750 \pm 50 \text{ ms}^{-1}$ in order to convert our seismic data to depth. The error with this variable can thus be expressed as a factor of average sediment thickness. We simplify our duration equation for the purposes of error propagation, duration (f) can be calculated using equation (5):

$$f \text{ (4 variables)} = \frac{A*T}{Th*S} \quad (5)$$

where A is the area of the GZW, and T is the average sediment thickness of the GZW (i.e. $A*T$ = GZW volume), divided by sediment flux ($Th*S$) where Th is deformation till thickness and S is

some variable paleo sediment flux / Th which accounts for all other variables contributing to paleo sediment flux. The variance of the duration ($\text{var}(f)$) can be calculated using equation (6):

$$\text{var}(f) = \sigma_A^2 \left[\frac{T}{Th \cdot S} \right]^2 + \sigma_T^2 \left[\frac{A}{Th \cdot S} \right]^2 + \sigma_{Th}^2 \left[\frac{A \cdot T}{S} * -\frac{1}{Th^2} \right]^2 + \sigma_S^2 \left[\frac{A \cdot T}{Th} * -\frac{1}{S^2} \right]^2 \quad (6)$$

where σ is standard deviation. Variance of f is thus the sum of the partial derivative of each variable (A, T, Th, S) calculated while holding all other variables constant. We assume a 5% σ for variables A and S to account for error in estimating GZW surface area, drainage area, and other factors contributing to sediment flux. We assume average sediment thickness (T) σ of 7.5% based on uncertainties concerning seismic sediment velocity and seismic resolution. σ for Th is by far the largest (23%) based on uncertainties concerning deformation till thickness (i.e. 6.5 ± 1.5 m).

We can then calculate the mean standard error of f with a 95% confidence interval using equation (7):

$$\text{Confidence Interval} = f \pm z * \sigma(f) \quad (7)$$

where z is the number of standard deviations from the mean needed to contain values within a confidence interval (i.e. 95% confidence interval, $z = 1.96$), and $\sigma(f)$ is equal to $\sqrt{\text{var}(f)}$.

VITA

Benjamin Joseph Krogmeier, a native of Plymouth, Michigan, graduated from Canton High School in 2009. He then attended Central Michigan University where he graduated with a Bachelor of Science in Geology in May 2014. Following graduation, Benjamin travelled to Minnesota where he completed his geology field camp through The University of Minnesota, Duluth. Benjamin then entered graduate school at Louisiana State University where he is a candidate to receive a Master of Science in Geology in May 2016. Upon graduating from LSU, Benjamin plans to find employment in the oil and gas industry.